Original Paper

Eletrônica de Potência
Open Journal of Power Electronics

Received April 25, 2025; accepted August 04, 2025; Date of publication August 27, 2025.
The review of this paper was arranged by Associate Editor Edivan L. C. da Silva and Editor-in-Chief Heverton A. Pereira.

Digital Object Identifier http://doi.org/10.18618/REP.e202550

A Fast Firing Angle Optimization Approach for Current-Controlled Switched Reluctance Generators in Wind Power Applications

Filipe P. Scalcon [1,*], Gustavo X. Prestes [2,3], Gaoliang Fang [4], Cesar J. Volpato Filho [5], Hilton A. Gründling [2], Rodrigo P. Vieira [2], Andrew M. Knight [1]

[1]University of Calgary, Calgary, Department of Electrical and Software Engineering, AB T2N 1N4, Canada
[2]Federal University of Santa Maria, Santa Maria, Power Electronic and Control Group, RS, Brazil
[3]Federal University of Roraima, Department of Electrical Engineering, Boa Vista, RR, Brazil
[4]University of Prince Edward Island, Faculty of Sustainable Design Engineering, Charlottetown, PEI C1A 4P3, Canada
[5]Siemens Gamesa Renewable Energy A/S, Brande, 7330, Denmark

e-mail: filipe.scalcon@ucalgary.ca*; gustavo.prestes@acad.ufsm.br; gfang@upei.ca; cesar.volpato@siemens-energy.com; ghilton03@gmail.com; rodrigo.vieira@ufsm.br; andyknight@ieee.org.
*Corresponding author.

ABSTRACT The adequate choice of excitation parameters is detrimental to the high performance operation of switched reluctance generators. Such task, however, is a complex problem which lacks solutions with simple analytical formulations. In this context, this paper presents a performance optimization procedure for switched reluctance generators operating in the current controlled region, below base speed. The proposal allows optimal firing angles to be determined based on the particle swarm optimization algorithm. A cost function is designed as a means to ensure performance with a compromise between reduced torque ripple and increased energy efficiency. A comparison with a traditional exhaustive search algorithm is provided, highlighting the reduced computational complexity of the proposal. Moreover, an original statistical analysis is presented as a means to demonstrate the low dispersion of the PSO-based procedure. Experimental results are provided in order to demonstrate the performance of the wind energy conversion system operating with optimal parameters.

KEYWORDS Firing angles, particle swarm optimization, switched reluctance generator, wind power.

I. INTRODUCTION

Switched reluctance generators (SRGs) present a simple structure, mechanical robustness, low manufacturing costs and an excellent fault tolerant capability. Moreover, the machine is suitable for application in hostile environments and capable of operating in a wide speed range [1]–[3]. The adoption of renewable energy sources, especially wind power, has increased significantly with the ever-growing concerns surrounding the environment and the use of fossil fuels. In this scenario, SRGs stand out as a suitable alternative for use in wind energy conversion systems (WECS) [4]–[9]. When compared to other alternatives, such as the doubly fed induction generators (DFIG) and permanent magnet synchronous generators (PMSGs), the SRG presents significant advantages. First, the SRG does not make use of permanent magnets or windings in the rotor of the machine, resulting in a considerably lower cost of acquisition [10]. Moreover, SRG-based WECS may present a structure without a gearbox, known as a direct-drive system. This topology presents increased reliability, given that it avoids the maintenance and failures that a gearbox potentially might endure. In addition, direct-drive wind turbines feature reduced weight and complexity [11]. The generators used in direct-drive systems, however, are low-speed high-torque machines, which often present lower efficiency when compared to high-speed generators [12]. Note that with adequate machine design, some of these issues may be mitigated [13]. Nevertheless, characteristics such as high torque ripple, acoustic noise production and a highly nonlinear behavior are among the main challenges of SRGs [14].

Unlike other electrical machines, the excitation interval of the SRG, given by the firing angles θ_{on} and θ_{off}, directly impacts the performance of the system. These parameters can be selected aiming to improve energy efficiency or reduce torque ripple, for example, which are both essential aspects to achieve a high performance SRG-based WECS [15]. However, the SRG presents a very complex and nonlinear model, hindering the use of simple analytical formulations to determine the optimal excitation interval. As a result, in recent years researchers have put significant effort in developing techniques for firing angle selection and performance optimization of SRGs [15]–[25].

In [15] a comprehensive discussion on the energy conversion process and control of SRGs is presented. An investiga-

tion on the impact of the firing angles on the machine is also conducted, evaluating the impact in variables such as the DC-link current. The author is able to demonstrate that different angle combinations can lead to the same output power, while showing very different torque ripple and efficiency metrics. The optimal performance of SRGs operating in the current-controlled region is the topic of investigation in [16]. A large number of simulations is performed in order to characterize the efficiency and torque ripple behavior with respect to the firing angles. As a solution, a simple controller making use of low complexity expressions for online turn-on and turn-off angle calculation is proposed. Given that the proposal of [16] was limited to operation below base speed, in [17] a similar study is carried out for SRGs operating with single-pulse control. Once more, a structure for optimal firing angle control is presented. The authors combine the proposals of [16] and [17] in [18], where a unified firing angle control approach for four quadrant operation in the entire speed range of the machine is described. Closed-loop angle control techniques, however, may lead to increased computational burden and augmented system complexity, given that additional controllers must be designed.

One alternative to avoiding closed-loop control techniques is the use of offline firing angle optimization strategies, such as exhaustive search approaches. These algorithms are able to successfully determine adequate excitation parameters while avoiding the need of any analytical formulations. Moreover, other advantages such as simplicity, evaluation of the entire search space and ensuring an optimal result is always found are also observed [8]. As such, several research studies have used an exhaustive search algorithm for SRG firing angle optimization [19]–[21]. In [19] extensive simulation is used in order to characterize the efficiency of the SRG as a function of the firing angles. Similarly, efficiency enhancement of an SRG is achieved in [20] through an iterative exhaustive search for optimal firing angles. In [21] dynamic simulations are used to optimize the performance of an SRG considering torque ripple, flux and current metrics. A sweeping approach is used and the optimal parameters are fitted to a high order polynomial for implementation. Exhaustive search strategies, however, have known drawbacks. Evaluating the entire search space often leads to a large computational burden. Moreover, depending on the number of parameters to be optimized or size of the search space, the approach may not be feasible [8].

The use of intelligent algorithms is a solution often employed for problems with complex formulation and that would otherwise require significant computational burden to be solved. These algorithms enable faster convergence and reduced computational complexity, given the entire search space does not need to be evaluated. As such, several researchers have proposed optimization procedures considering superior optimization techniques [22]–[25]. In [22] a genetic algorithm is used in order to determine the optimal firing angles of an SRG. A multi-objective performance optimization for SRGs in single pulse operation is presented in [23], where a three-term cost function is adopted. In similar fashion, the design of computational experiments is employed in [24] for a multi-objective performance optimization of an SRG-based WECS. A normalized cost function containing torque, flux and current metrics is adopted and optimization is performed for operation below and above base speed. The same procedure is also employed for the system used in [25].

Another popular metaheuristic for engineering problems is the particle swarm optimization (PSO) algorithm, proposed by [26]. In this context, an optimization procedure for the firing angles of SRGs operating in the current-controlled region based on the PSO algorithm is proposed in [27]. A traditional exhaustive search approach is detailed and then compared to the proposed PSO strategy. The proposal is capable of significant reduction in computational burden while also enabling a simple digital implementation through a linear regression, avoiding memory intensive lookup tables. In this regard, this paper can be seen as an extension of [27]. Once more, seeking to ensure a balance of reduced torque ripple and improved energy efficiency, a two-term normalized cost function is chosen. Unlike the original proposal, the computational efficiency of the PSO procedure is further highlighted in this paper. Moreover, a statistical analysis is presented as a means to demonstrate the low dispersion and high repeatability of the proposed method, something not presented previously in literature for SRG firing angle optimization. Lastly, experimental results are provided, demonstrating the performance of the system with the proposed control strategy under different operating conditions.

The main contributions of this paper can be summarized as follows:

1) A systematic and straightforward PSO-based firing angle optimization strategy for SRGs in wind power applications. Compared to other strategies, the proposal presents significantly reduced computational complexity, enabling a faster design stage.
2) Due to the design choices of using an optimal power profile and a fixed DC-link voltage, the proposal is able to achieve a simple digital implementation, avoiding the use of lookup tables, as well as any additional hardware or complex controllers.
3) A statistical analysis of the results through the use of a dispersion metric, demonstrating the adequate convergence, and high repeatability of the proposal, something not previously presented in SRG literature.

II. SRG-BASED WIND ENERGY CONVERSION SYSTEM

In a wind turbine the mechanical power, P_m, is given by

$$P_m = \frac{1}{2}\pi\rho C_p\left(\lambda,\beta\right)R^2V^3 \tag{1}$$

where ρ is the air density, $C_p\left(\lambda,\beta\right)$ is power coefficient of the wind turbine , λ is the tip speed ratio, β is the blade pitch angle, R is the rotor radius and V is the wind speed [28].

Variable speed operation is an effective way of increasing the energy efficiency of wind turbines operating below the rated speed [4]. As such, the optimal output power profile for the studied WECS is given by

$$P_{opt} = k_{opt}\omega_r^3 \tag{2}$$

where P_{opt} is the optimal output power, k_{opt} is a coefficient related to the blade aerodynamics and ω_r is the rotor speed. Determining the value of k_{opt} can be a complex task, however, given that the machine used for this paper has a construction and rated values identical to the one used in [7], [24], the same coefficient value of $k_{opt} = 5.16 \times 10^{-4}$ will be adopted. Then, considering the value of k_{opt} in (2), the optimal power curve of the system as a function of rotor speed can be obtained, as shown in Fig. 1. Please note that the proposed procedure is intended for the current-controlled region, where a hysteresis regulator is used, detailed below.

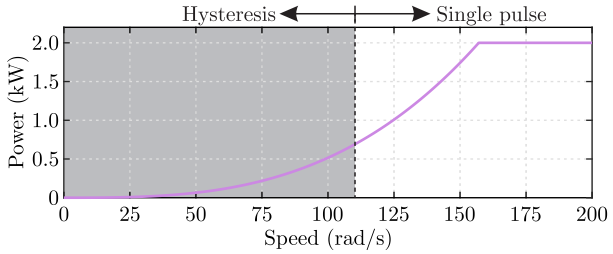

FIGURE 1. Optimal output power curve for the studied system.

Considering the highly nonlinear behavior of the SRG, a simple mathematical formulation cannot be used to express the generated power of the machine. By taking some assumptions into consideration, a simplified formulation can be attained. Hence, the average output power can be described by [24]

$$P_{out} = \frac{N_s N_r V_{DC}^2}{\omega_r}\left(\int_{\theta_{on}}^{\theta}\frac{(\theta-\theta_{on})}{L(\theta)}d\theta + \int_{\theta_{on}}^{\theta}\frac{(\theta_{off}-\theta-\theta_{on})}{L(\theta)}d\theta\right) \tag{3}$$

where N_s is the number of stator poles, N_r is the number of rotor poles, V_{DC} is the DC-link voltage, θ_{on} is the turn-on angle, θ_{off} is the turn-off angle, θ is the rotor position and $L(\theta)$ is the phase inductance as a function of the rotor position.

The effect of the firing angles, the DC-link voltage and the rotor speed on the output power of the SRG is made evident by (3). Considering the DC-link voltage value on the optimization procedure, however, would increase the complexity of the optimization problem, as a third variable would be introduced. Moreover, grid connected converters (GCC) often require a sufficiently high and stable DC-link voltage [25]. Therefore, it is a reasonable design choice for this paper to consider a fixed value of 400 V for the DC-link voltage, as it is often considered for converters tied to a 120 V grid [29], [30]. It should be noted that some papers in the literature optimize the DC-link voltage [24], [25], nonetheless, note that the same papers make use of additional DC-DC converters in order to step-up voltage for the GCC. In this context, by using a fixed DC-link voltage the proposal reduces the cost of the system, avoiding the need for additional hardware, as well as the control complexity, circumventing the use of multiple controllers.

III. PARTICLE SWARM OPTIMIZATION

The particle swarm optimization is a metaheuristic inspired in the intelligence of groups observed in nature, such as flocks of birds and schools of fish. It was first proposed by [26], being an efficient tool for solving complex optimization problems. The PSO presents some advantages over other optimization algorithms, such as effortless implementation, robustness, no requirements of derivative calculation, among others. When compared to an exhaustive search, specifically, the PSO approach delivers significantly improved computational efficiency, given that the entire search space does not need to be evaluated. It should be noted that adequate configuration parameters are required for the best performance of the PSO algorithm [31], [32].

The PSO algorithm consists of a set of N particles being initially randomly placed on the search space. At each iteration the speed of the particles is updated based on the individual and global knowledge, i.e. the minimum value known by the particle and minimal value known by the swarm, respectively. Typically, the algorithm is terminated after a set number of M epochs, i.e. iterations, is executed and the global minimum then is returned as the optimal solution. Several variations of the PSO have been proposed since it was first proposed, seeking to improve different aspects algorithm [33]. The variation of the PSO algorithm used in this paper can be summarized by the following steps:

1) The PSO algorithm is configured, where parameters such as number of particles, number of epochs, social and cognitive coefficients are set;
2) The position of each of the particles is randomly initialized to values within the search space;
3) The cost function is evaluated for every particle with respect to its current position;
4) The cost function values are compared to the ones calculated in the previous iteration. If the cost is lower than the minimum particle known value, $P_{x.best}$, this value is updated. Moreover, if any of the particles finds a cost lower than the minimum global known value, G_{best}, this value is also updated;
5) The speed of every particle is updated according to the following equation:

$$v_x(k+1) = \lambda v_x(k) + \psi_1 r_1 (P_{x.best} - s_x(k)) + \psi_2 r_2 (G_{best} - s_x(k)). \tag{4}$$

where $v_x(k)$ is the speed of a given particle in a given epoch and λ is the inertia coefficient, used as a means to slow down the movement of particles with

the passing of epochs. Sub-index x is used to indicate the particle number, where $\{x \in \mathbb{N} : x > 0\}$, while sub-index k is used to indicate the epoch number, where $\{k \in \mathbb{N} : k > 0\}$. Parameters ψ_1 and ψ_2 are the cognitive and social coefficients, respectively. Terms r_1 and r_2 are functions that return a randomly generated value with amplitude between 0 and 1 [31].

6) The position of every particle is updated according to the following equation:

$$s_x\left(k+1\right) = s_x\left(k\right) + v_x\left(k+1\right) \tag{5}$$

where $S_x\left(k\right)$ is the speed of a given particle in a given epoch.

7) The algorithm repeats steps 2) to 6) until the stopping criteria is met, in this case, the set number of epochs.
8) The best global known value at the end of execution, G_{best}, is returned as the solution of the PSO.

In the following Section, two SRG firing angle optimization procedures will be presented.

IV. SRG FIRING ANGLE OPTIMIZATION

This Section presents two optimization procedures for the firing angles of an SRG operating below base speed, in the current-controlled region. As can be observed in (3), the adequate selection can significantly impact the generated power, as well as other parameters that directly impact performance of the WECS. Note that for full-range operation, a single-pulse control algorithm as well as a transition strategy must be implemented, however, this is outside of the scope of the paper.

The proposed optimization algorithms make use of sequential dynamic simulations. For that, a model is built in MATLAB/Simulink® as depicted in [34]. The machine used in this paper has a 12/8 3-phase configuration. Moreover, the machine has a rated power of 2 kW and a rated speed of 157 rad/s, with a base speed of 110 rad/s. An asymmetric half-bridge (AHB) converter is used to drive the SRG. The control structure used is presented in the form of a block diagram in Fig. 2. A cascaded control structure is implemented, where an outer loop voltage controller and an inner loop current controller are used. The voltage control is performed by means of a sliding mode controller, detailed in [35], [36]. Current control is carried out using a hysteresis regulator, where only the positive and negative voltage converter states are used, characterizing hard-chopping operation.

In order to guide the optimization algorithms, a cost function is necessary. Given that this paper seeks to achieve a balance between reduced torque ripple and improved energy efficiency, the cost function, $F\left(\theta_{on}, \theta_{off}\right)$, can be written as

$$F\left(\theta_{on}, \theta_{off}\right) = \bar{T}_{ripple} + \bar{i}^2_{rms} \tag{6}$$

where $\bar{T}_{ripple}$ is the normalized torque ripple value and $\bar{i}^2_{rms}$ is the normalized square RMS current value in phase "a". The values are normalized by dividing any given value by the maximum observed value inside the evaluated search space

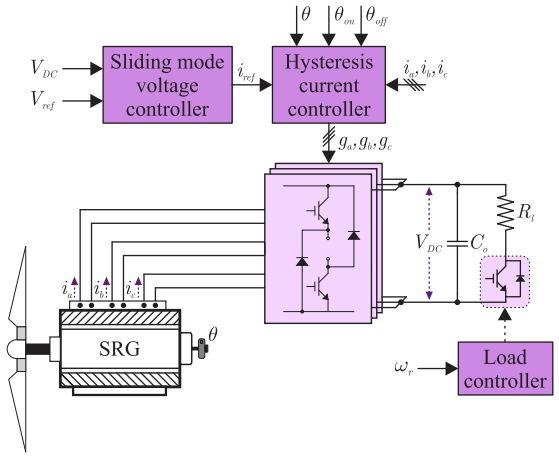

FIGURE 2. Block diagram of the control structure.

for that particular metric. Torque ripple, T_{ripple}, is calculated as,

$$T_{ripple} = \frac{T_{\max} - T_{\min}}{T_{avg}} \tag{7}$$

where $T_{\max}$ is the maximum torque value, $T_{\min}$ is the minimum torque value and T_{avg} is the average torque value within a particular operating condition.

Remark 1:
The load connected to the SRG also affects the optimal excitation parameters of the machine. Therefore, an optimization procedure should consider both different speed and load conditions. This would yield a lookup table of optimal firing angles which is dependent of speed and load, increasing complexity and requiring meaningful memory allocation [37]. For this paper, however, note that an optimal power output profile is adopted, where for any given rotor speed condition, only an optimal load value is considered. Therefore, the proposal is less computationally intensive and leads to a simpler digital implementation. Operation under transient load conditions will lead to sub-optimal performance, however, note this corresponds to a minor part of the operation of the wind turbine and the above-listed benefits outweigh minor performance losses, as depicted in [37].

Remark 2:
The RMS current value is often considered in the cost functions of similar proposals, such as [21], [24], as a means to account for energy efficiency. In this proposal, however, the cost function is designed considering the square of this value, $\bar{i}^2_{rms}$. This is justified by the following reasons: i) the squared RMS value better reflects the copper losses in the WECS. ii) by squaring the values, the difference between similar value points becomes more apparent, which in turn facilitates the optimization procedure.

Remark 3:

Some SRG optimization proposals have included a peak flux linkage term in the cost function, in order to account for iron losses. It should be noted, however, that in the current-controlled region copper losses are prevalent, with iron losses only being more prominent at high-speed operating conditions. Moreover, reducing the RMS current value is a sufficient approach, given that it also leads to a reduction in the peak flux linkage value [15]. In this context, it is a reasonable design choice to not include the flux linkage value in the cost function for this paper.

Remark 4:
Although equal weight is given to both of the normalized terms in the cost function, note that different values can be considered, enabling the designer to steer the performance of the SRG towards lower torque ripple or increased energy efficiency, for example.

Two different firing angle optimization procedures will be detailed in the following subsections. The first technique is based on an exhaustive search optimization approach, while the second technique is based on the PSO algorithm.

A. Exhaustive search optimization procedure

Fig. 3 presents the flowchart of the exhaustive search optimization procedure. The SRG model described at the start of this Section is used, along the configuration parameters given in Table 1.

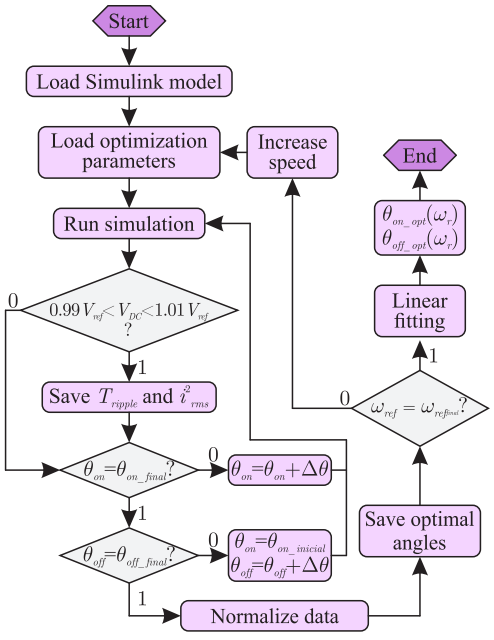

FIGURE 3. Flowchart of the exhaustive search optimization procedure.

Initially, the machine data are loaded into Simulink®, i.e. the current and torque lookup tables. Following this, the exhaustive search configuration parameters are also set. Simulation process starts for the first desired speed value,

TABLE 1. Exhaustive search optimization parameters.

Parameter	Value
Speed interval	[60,100] rad/s
Speed step	10 rad/s
θ_{on} bounds	[35°,44°]
θ_{off} bounds	[12°,21°]
θ increment	0.25°

where all of the possible angle combinations are tested. At the end of each simulation, the DC-link voltage value is measured. If the average value is within $\pm 1\%$ of the reference value, then measured torque ripple and RMS current metrics are stored. On the contrary, if the reference value is not reached, the particular angle combination is excluded from the optimization procedure. Note that all measurements are performed after the system has reached a steady state condition.

Once a simulation is finished and the decision of storing the performance metrics is made, the firing angles are incremented and the simulation process is resumed. This is repeated until the last combination within the search space is evaluated, that is, $\theta_{on} = \theta_{on\_final}$ and $\theta_{off} = \theta_{off\_final}$. Once every measurement is obtained, the maximum values are located and the normalization of the torque and current metrics is performed. With the normalized values, the cost function (6) is computed for every angle combination, and parameters that lead to the lowest cost are located. These angles are then saved as the optimal firing angles for that particular speed. The cost function values for a speed of 80 rad/s are presented in Fig. 4. For this condition, the optimal firing angles are $\theta_{on} = 39.5°$ and $\theta_{off} = 17.75°$.

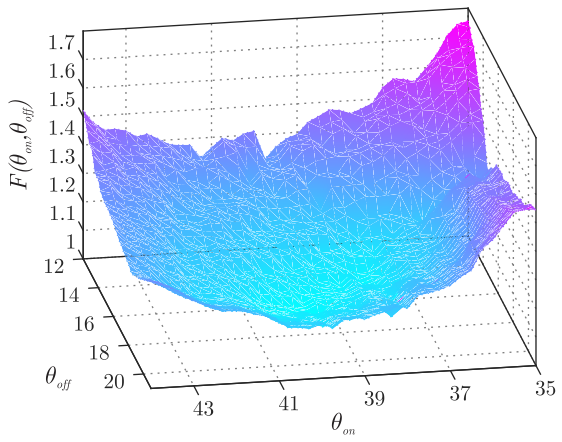

FIGURE 4. Cost function values for the search space at a speed of 80 rad/s.

The optimization process is continued by incrementing the speed value and repeating the simulation process described previously. Once every speed value has been assessed, the optimal firing angles are fitted to a linear regression. This enables a straightforward, yet effective digital implementation. The resulting optimal firing angles for operation in the

current-controlled region for the adopted system are given by

$$\begin{aligned} \theta_{on\_opt}(\omega_r) &= -0.145\,|\omega_r| + 50.95 \\ \theta_{off\_opt}(\omega_r) &= 17.10. \end{aligned} \tag{8}$$

A total of 6845 simulations were performed during the execution of the exhaustive search optimization procedure, with a total execution time of 250.13 minutes on an Intel Core i7 laptop with 16GB of RAM.

Remark 5:
Although a linear regression is proposed, note that $\theta_{off\_opt}(\omega_r)$ is expressed as a fixed value. This is justified by the fact that the regression resulted in a line with a very small linear coefficient, with a magnitude inferior to 10^{-3}. Hence, the turn off angle would present an unnoticeable variation with respect to speed in the desired speed interval. Therefore, the value is considered a constant as a simplifying measure, given that implementing the resulting regression will lead to no measurable performance improvement. Please note, however, that this is not a general rule and may not be true for different SRGs.

B. PSO-based optimization procedure

Fig. 5 presents the flowchart of the proposed particle swarm optimization procedure. Once more, the SRG model described at the start of this Section is used, along with the configuration parameters given in Table 2. The number of epochs and particles has been chosen based on a preliminary analysis, where the values are chosen as a means to strike a balance between low computational burden and good convergence [27]. The cognitive and social coefficient values are chosen based on guidelines presented in [26], and are assigned equal values to avoid both excessive wandering ($\psi_1 \gg \psi_2$) and premature convergence to local minima ($\psi_1 \ll \psi_2$). For the remaining parameters, the same reasoning from the exhaustive search optimization procedure is considered.

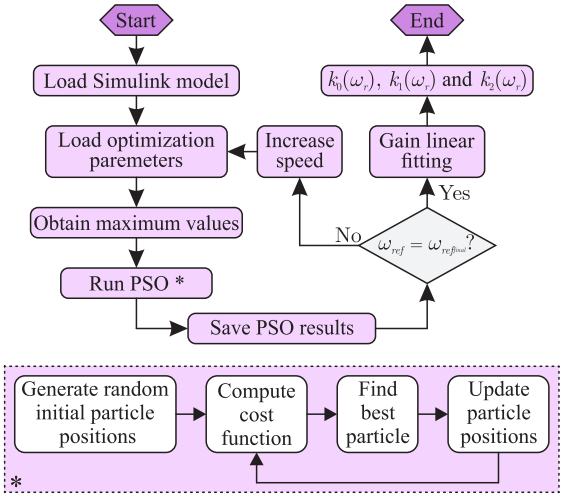

FIGURE 5. Flowchart of the PSO-based procedure.

TABLE 2. PSO parameters.

Parameter	Value
Speed interval	[60,100] rad/s
Speed step	10 rad/s
θ_{on} bounds	[35°,44°]
θ_{off} bounds	[12°,21°]
Number of particles	5
Number of epochs	25
Cognitive coefficient	0.5
Social coefficient	0.5

The procedure is initiated by loading the SRG lookup tables and the parameters for the PSO algorithm, such as the speed and firing angle search space. Subsequently, two simulations are performed, with the objective of obtaining the maximum current and torque ripple metrics for the desired search space. These values are obtained in advance in order to enable normalization of the cost function, which must be performed at the end of each simulation, given the nature of the PSO algorithm [27]. Then, the execution of the PSO algorithm starts. At the end of each simulation, performed based on the position of each particle in a given epoch, the output voltage is measured. If the average value is within $\pm 1\%$ of the reference value, the cost function value is calculated. If not, a value of $F(\theta_{on}, \theta_{off}) = 1000$ is assigned, indicating to the PSO algorithm that the evaluated angle combination is not appropriate. Once the stop criteria is reached, in this case the set number of epochs, the best known result by the swarm is stored as the optimal firing angles for the evaluated speed.

Simulation results for the PSO algorithm at four different epochs for a speed of 80 rad/s are presented in Fig. 6. The cost function values obtained in Fig. 4 are plotted in the background, in the form of contours. It can be seen that with the passing of the epochs the particles move through the search space and converge towards the global minimum. The results are very similar to the exhaustive search method, sometimes being even slightly superior, while performing a significantly lower number of simulations.

The evolution of the best known cost function value through the epochs is presented in Fig. 7. Once again, the convergence of the algorithm can be observed.

Much like the exhaustive search approach, the PSO-based procedure is repeated until every desired speed value has been assessed. Then, a linear regression is performed with respect to speed as a means to fit the optimal firing angle values to a straight line. The resulting optimal firing angles of the PSO procedure are given by

$$\begin{aligned} \theta_{on\_opt}(\omega_r) &= -0.145\,|\omega_r| + 51.57 \\ \theta_{off\_opt}(\omega_r) &= 17.11. \end{aligned} \tag{9}$$

A total of 635 simulations were carried out during the execution of the PSO-based procedure, resulting in a 90.72% reduction of the computational burden when compared to the

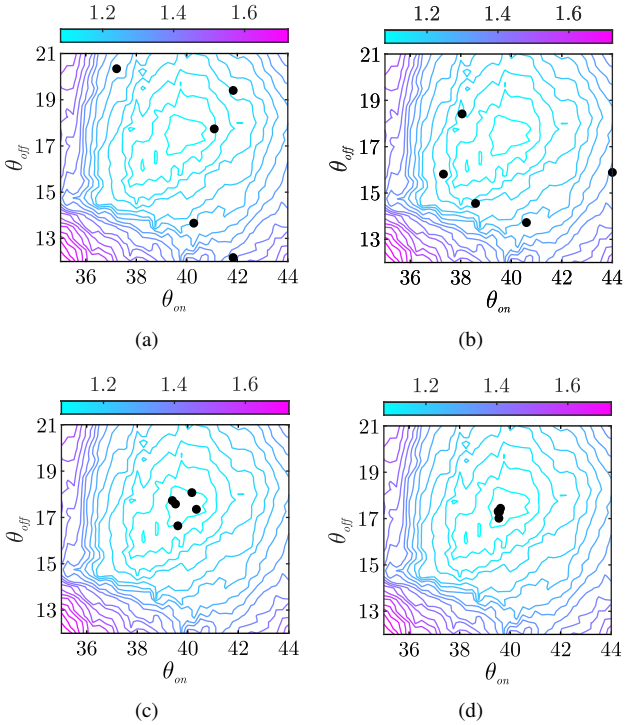

FIGURE 6. Particle positions through the epochs. (a) Epoch 1. (b) Epoch 5. (c) Epoch 15. (d) Epoch 25.

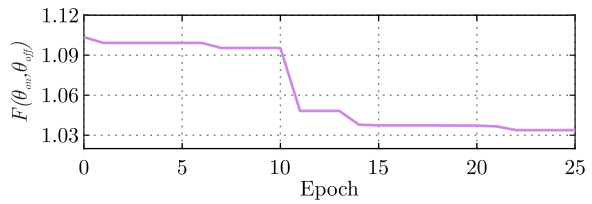

FIGURE 7. Evolution of cost function value over the epochs.

exhaustive search optimization procedure. The total execution time was 56.77 minutes on the same Intel Core i7 laptop with 16GB of RAM.

Once more, the turn off angle is implemented as a fixed value. Please refer to *Remark 4* for the reasoning.

C. Results comparison

Table 3 shows the optimal firing angles as well as the lowest cost function value obtained by the exhaustive search and PSO algorithms, respectively.

First, it can be seen that both techniques have found very similar results for the optimal firing angles. Moreover, it can be observed that the cost function values of the results found by the PSO procedure are often smaller than those found by the exhaustive search approach, indicating that a point of superior performance has been located. This is justified by the fact that the PSO particles can assume any value within the search space, while the exhaustive search strategy is limited by the predefined angle increments. Lastly, it should be noted that the results of the PSO may vary due

TABLE 3. Optimization results for the exhaustive search and PSO procedures.

	Fine grid			PSO		
ω_r (rad/s)	θ_{on} (°)	θ_{off} (°)	Cost	θ_{on} (°)	θ_{off} (°)	Cost
60	43.00	17.50	0.9697	43.00	17.20	0.9678
70	39.75	16.25	0.9527	41.17	17.07	0.9570
80	39.50	17.75	1.0477	39.55	17.02	1.0339
90	37.75	16.75	1.1537	39.27	17.12	1.1340
100	36.75	17.25	1.1372	36.68	17.14	1.1324

to the random nature of the algorithm. Moreover, they are dependent on an adequate number of particles and epochs in order to ensure convergence. However, with a large enough swarm for a large enough number of epochs, convergence should not be an issue.

Fig. 8 shows the optimal angles and the linear regressions obtained by both optimization procedures. Once more, it should be noted that the results present a similar behavior, with the PSO showing significantly reduced computational burden and slightly improved performance, given the lower cost function values found. Moreover, turn off angles are considered fixed for both methods, given the negligible variation the linear regressions have shown with respect to speed (refer to *Remark 4*).

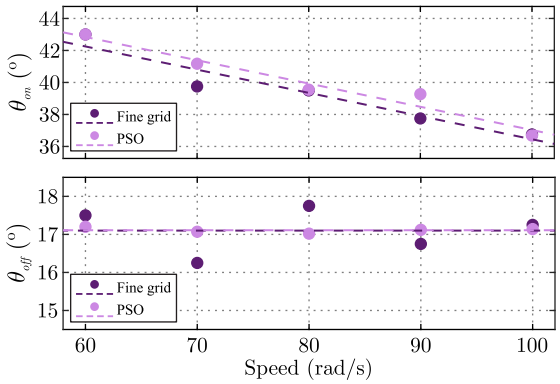

FIGURE 8. Comparison of the optimal angles and linear regressions obtained by both optimization procedures.

D. Statistical analysis

As previously mentioned, the PSO algorithm presents a random nature. The initial position of particles is randomly selected and two terms of (4), r_1 and r_2, persistently introduce random disturbances in the movement of particles. As such, it is expected that the results of an optimization procedure based on this algorithm will vary. A sufficiently large number of particles and epochs, however, should ensure that the procedure achieves convergence repeatedly. In order to verify the dispersion of the results obtained by the proposal, the PSO-based procedure was executed 100 times for the same speed value. Note that the random number generation of the

initial values is handled by the PSO function available in MATLAB. It is then possible to calculate the coefficient of variation of the saved optimal turn on and turn off angles, as well as the cost function value, according to

$$CV = \frac{\sigma}{\mu}\,, \tag{10}$$

where CV is the coefficient of variation, σ is the standard deviation and μ is the average. The results are shown in (11) for a speed of 80 rad/s and in (12) for a speed of 100 rad/s.

$$\begin{aligned} CV_{\theta_{on}} &= 0.64\% \\ CV_{\theta_{off}} &= 1.88\% \\ CV_{F(\theta_{on},\theta_{off})} &= 0.57\% \end{aligned} \tag{11}$$

$$\begin{aligned} CV_{\theta_{on}} &= 0.76\% \\ CV_{\theta_{off}} &= 2.42\% \\ CV_{F(\theta_{on},\theta_{off})} &= 0.625\% \end{aligned} \tag{12}$$

where $CV_{\theta_{on}}$ is the coefficient of variation of the turn-on angle, $CV_{\theta_{off}}$ is the coefficient of variation of the turn-off angle and $CV_{F(\theta_{on},\theta_{off})}$ is the coefficient of variation of the cost function.

It can be seen that a low dispersion is verified within the results, indicating that the proposed PSO procedure presents good convergence and repeatability, even for different speed values.

V. EXPERIMENTAL RESULTS

Experimental results are presented in this Section in order to validate the effectiveness of the proposed firing angle optimization strategy. The characteristics of the machine are detailed at the start of Section III. The experimental setup is presented in Fig. 9. It is composed of an SRG, a three-phase AHB converter, an induction motor (IM) controlled by a commercial inverter, used as a prime mover, and a resistor bank, used as a load.

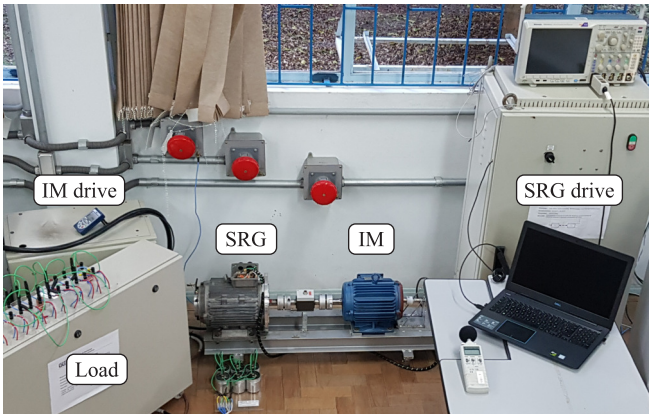

FIGURE 9. Experimental setup encompassing the SRG, an IM used as a prime mover, the drive for both machines and the electrical load.

Fig. 10 shows the block diagram of the proposed control strategy applied to a SRG-based WECS. A TMS320F28335 digital signal processor (DSP) is used for digital implementation, with a sampling frequency of $f_s = 30$ kHz. As mentioned in Section IV, a sliding mode voltage controller is used along with an inner loop hysteresis current regulator implemented using hard chopping and a hysteresis band of 100mA. The small band value is used to ensure reduced current ripple and, in turn, help decrease torque ripple. The voltage reference is kept at 400 V for all tests [38]. The optimal firing angles are implemented according to the results obtained in (9). Instantaneous torque measurements are carried out inside of the DSP with the use of a torque lookup table containing characteristics of the switched reluctance machine used. A controllable switch is connected in series with the resistive load. A PWM signal with variable duty cycle is used as a means to control the output power as a function of speed, according to the optimal profile presented in (2). The duty cycle is given by

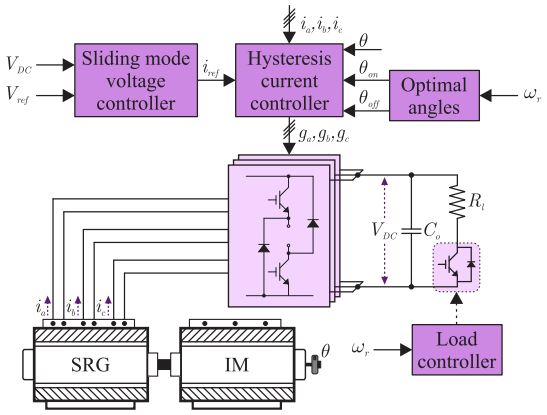

FIGURE 10. Block diagram of the SRG control strategy used for experimental validation.

$$d_{cycle} = \frac{R_l}{\left(\frac{V_{DC}^2}{P_{opt}}\right)}. \tag{13}$$

where $R_l = 270\Omega$.

A. Dynamic performance

In order to evaluate the dynamic performance of the proposal, inherent in the operation of WECS, Fig. 11 shows the experimental results of the proposed control strategy in a variable speed test. The speed of the IM is initially set to 60 rad/s, and then, at $t = 3.5$s, it is increased in a ramp until reaching the speed of 100 rad/s, at $t = 4.5$s.

It is observed from Fig. 11(a) that the system presents suitable reference tracking, given that the output voltage of the SRG is regulated at 400 V throughout the test. Moreover, it can be seen that current amplitude increases during the test, as expected given the optimal output power profile. Similarly, Fig. 11(b) shows that the power output of the system is increased along with the increase in rotor speed. Lastly, it can be seen that the firing angles are dynamically adjusted

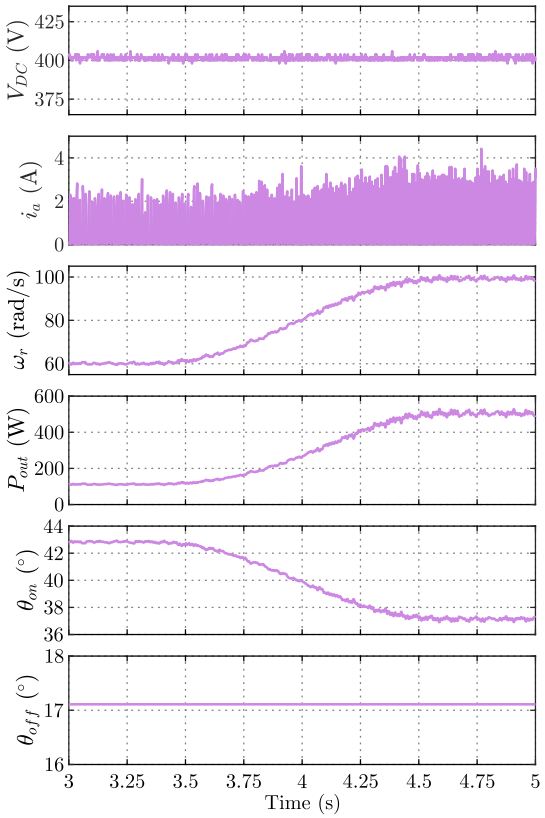

FIGURE 11. Experimental results for a variable speed condition. Measurements of DC-link voltage, phase current, rotor speed, output power and firing angles, respectively.

according to (9). This enables the system to operate with reduced torque ripple and increased energy efficiency.

B. Steady-state performance

In order to verify the steady-state performance of the system, experimental results at the speeds of 80 rad/s and 100 rad/s are presented in Figs. 12 and 13, respectively. Three different firing angle conditions were considered: the angles obtained from the proposed PSO-based optimization procedure (case 1), the angles obtained from the exhaustive search optimization procedure (case 2) and the angles obtained from the exhaustive search optimization procedure considering only the square RMS current value as the cost function (case 3).

Initially, it is observed that the reference voltage is adequately tracked by the sliding mode controller in all cases. Moreover, it can be seen that the experimental results for case 1 and case 2 are very similar, as expected from the analysis show in subsection IV-C. Case 3 shows a reduction in the RMS current value, given the shorter excitation interval. Note, however, that a significantly larger torque ripple value is observed when compared to the proposed approach. This is especially undesirable, as it can lead to premature mechanical wear. Lastly, one can observe that the experimental results for case 1 are consistent with the simulation values obtained in [27].

A numerical analysis is presented in Table 4, where torque ripple and RMS current measurements are presented for the three cases in both speed conditions.

TABLE 4. Torque ripple and RMS current comparison for the different firing angle cases.

	80 rad/s		100 rad/s	
	T_{ripple}	i_{RMS}	T_{ripple}	i_{RMS}
Case 1	133.37%	1.545 A	111.70%	2.015 A
Case 2	131.88%	1.544 A	113.85%	2.007 A
Case 3	229.02 %	1.497 A	168.01%	1.853 A

Once more, it can be seen that the proposed procedure (case 1) exhibits nearly identical performance to the exhaustive search approach (case 2), while still presenting the aforementioned advantages of the proposal. Furthermore, it is again observed that optimizing the RMS current (case 3) reduces its value, nonetheless, at the cost of significantly increased torque ripple when compared to the proposal (case 1).

VI. CONCLUSION

In this paper, a procedure to optimize the firing angles of an SRG operating in a variable speed condition is proposed. The algorithm is intended for SRG operating under current control, below base speed. A normalized cost function is used as a means to account for two different variables, in this case torque ripple and squared RMS current. When compared to a conventional exhaustive search algorithm, the PSO-based procedure is capable of locating equivalent or better optimal firing angles, while reducing computational burden by approximately 90.27%. Experimental results are provided to attest the effectiveness of the proposed WECS operating with the optimized firing angles. It should be noted that the proposed procedure can be used as a framework for future performance optimization approaches, through the use of different cost functions.

ACKNOWLEDGMENT

This study was financed in part by in part by Coordenação de Aperfeiçoamento de Pessoal de Nível Superior – Brasil (CAPES/PROEX) – Finance Code 001, and in part by Conselho Nacional de Desenvolvimento Científico e Tecnológico - Brasil (CNPq) - processo 305211/2025-0.

AUTHOR'S CONTRIBUTIONS

F.P.SCALCON: Conceptualization, Investigation, Methodology, Writing – Original Draft, Writing – Review & Editing. **G.X.PRESTES:** Investigation, Validation. **G.FANG:** Investigation, Writing – Review & Editing. **C.J.V.FILHO:** Investigation, Writing – Review & Editing. **H.A.GRÜNDLING:** Funding Acquisition, Project Administration, Supervision, Writing – Review & Editing. **R.P.VIEIRA:** Conceptualization, Funding Acquisition, Project Administration, Supervi-

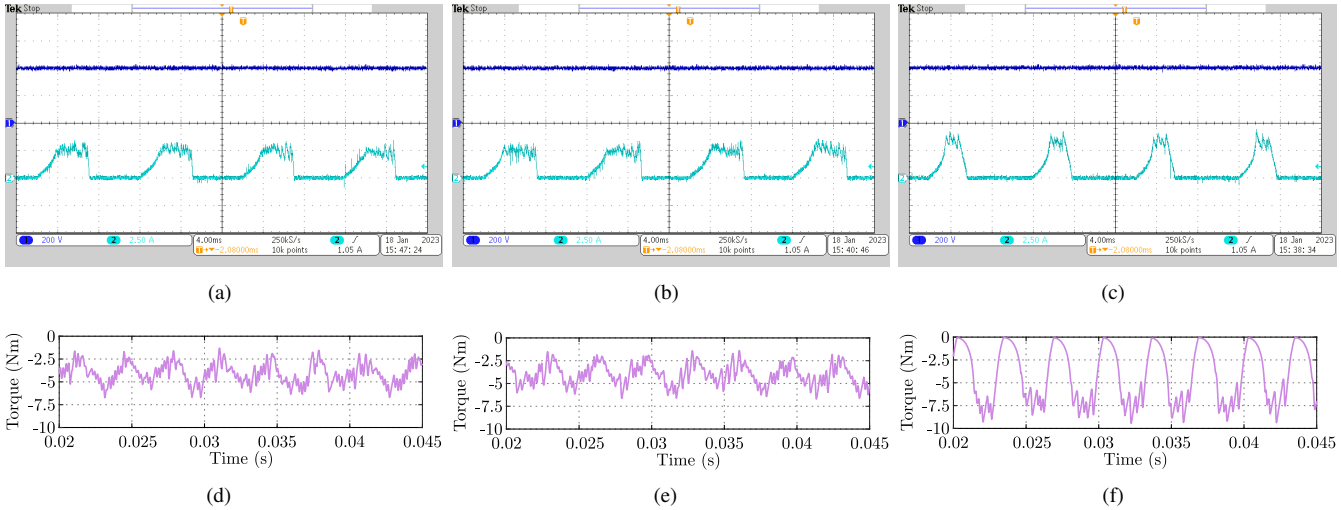

FIGURE 12. Experimental results for a speed of 80 rad/s. DC-link voltage and phase current for (a) Case 1, (b) Case 2 and (c) Case 3. Torque for (d) Case 1, (e) Case 2 and (f) Case 3.

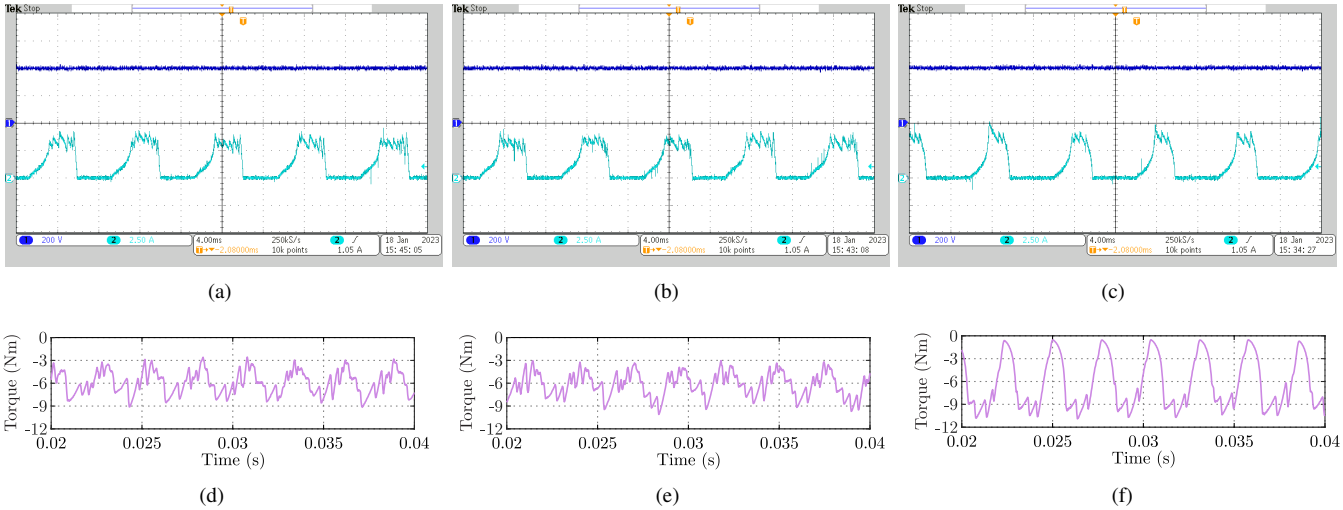

FIGURE 13. Experimental results for a speed of 100 rad/s. DC-link voltage and phase current for (a) Case 1, (b) Case 2 and (c) Case 3. Torque for (d) Case 1, (e) Case 2 and (f) Case 3.

sion, Writing – Review & Editing. **A.M.KNIGHT:** Funding Acquisition, Supervision.

PLAGIARISM POLICY

This article was submitted to the similarity system provided by Crossref and powered by iThenticate – Similarity Check.

DATA AVAILABILITY

The data used in this research is available in the body of the document.

REFERENCES

[1] B. Bilgin, B. Howey, A. D. Callegaro, J. Liang, M. Kordic, J. Taylor, A. Emadi, "Making the Case for Switched Reluctance Motors for Propulsion Applications", *IEEE Transactions on Vehicular Technology*, vol. 69, no. 7, pp. 7172–7186, 2020, doi:10.1109/TVT.2020.2993725.

[2] L. Ge, J. Zhong, C. Bao, S. Song, R. W. De Doncker, "Continuous Rotor Position Estimation for SRM Based on Transformed Unsaturated Inductance Characteristic", *IEEE Transactions on Power Electronics*, vol. 37, no. 1, pp. 37–41, 2022, doi:10.1109/TPEL.2021.3096738.

[3] A. Verma, S. S. Ahmad, G. Narayanan, "Optimal Control of Single-Pulse-Operated Switched Reluctance Generator to Minimize RMS Phase and RMS DC-Bus Current", *IEEE Transactions on Industry Applications*, vol. 60, no. 1, pp. 507–519, 2024, doi:10.1109/TIA.2023.3327977.

[4] R. Cardenas, R. Pena, M. Perez, J. Clare, G. Asher, P. Wheeler, "Control of a switched reluctance generator for variable-speed wind energy applications", *IEEE Transactions on Energy Conversion*, vol. 20, no. 4, pp. 781–791, 2005, doi:10.1109/TEC.2005.853733.

[5] Y.-C. Chang, C.-M. Liaw, "On the Design of Power Circuit and Control Scheme for Switched Reluctance Generator", *IEEE Transactions on Power Electronics*, vol. 23, no. 1, pp. 445–454, 2008, doi:10.1109/TPEL.2007.911872.

[6] E. Echenique, J. Dixon, R. Cardenas, R. Pena, "Sensorless Control for a Switched Reluctance Wind Generator, Based on Current Slopes and Neural Networks", *IEEE Transactions on Industrial Electronics*, vol. 56, no. 3, pp. 817–825, 2009, doi:10.1109/TIE.2008.2005940.

[7] T. A. d. S. Barros, P. J. d. S. Neto, P. S. N. Filho, A. B. Moreira, E. R. Filho, "An Approach for Switched Reluctance Generator in a Wind Generation System With a Wide Range of Operation Speed", *IEEE Transactions on Power Electronics*, vol. 32, no. 11, pp. 8277–8292, 2017, doi:10.1109/TPEL.2017.2697822.

[8] F. P. Scalcon, G. Fang, C. J. V. Filho, H. A. Gründling, R. P. Vieira, B. Nahid-Mobarakeh, "A Review on Switched Reluctance Generators in Wind Power Applications: Fundamentals, Control and Future Trends", *IEEE Access*, vol. 10, pp. 69412–69427, 2022, doi:10.1109/ACCESS.2022.3187048.

[9] V. Narayanan, B. Singh, "Wind-Driven Position Sensorless Switched Reluctance Generator and Diesel Generator Based Microgrid for Optimal Fuel Consumption and Power Blackout Mitigation", *IEEE Transactions on Industrial Electronics*, vol. 71, no. 4, pp. 3660–3672, 2024, doi:10.1109/TIE.2023.3279561.

[10] E. Bostanci, M. Moallem, A. Parsapour, B. Fahimi, "Opportunities and Challenges of Switched Reluctance Motor Drives for Electric Propulsion: A Comparative Study", *IEEE Transactions on Transportation Electrification*, vol. 3, no. 1, pp. 58–75, 2017, doi:10.1109/TTE.2017.2649883.

[11] M. M. Namazi, S. M. S. Nejad, A. Tabesh, A. Rashidi, M. Liserre, "Passivity-Based Control of Switched Reluctance-Based Wind System Supplying Constant Power Load", *IEEE Transactions on Industrial Electronics*, vol. 65, no. 12, pp. 9550–9560, 2018, doi:10.1109/TIE.2018.2816008.

[12] H. Polinder, J. A. Ferreira, B. B. Jensen, A. B. Abrahamsen, K. Atallah, R. A. McMahon, "Trends in Wind Turbine Generator Systems", *IEEE Journal of Emerging and Selected Topics in Power Electronics*, vol. 1, no. 3, pp. 174–185, 2013, doi:10.1109/JESTPE.2013.2280428.

[13] M. Abdalmagid, E. Sayed, M. H. Bakr, A. Emadi, "Geometry and Topology Optimization of Switched Reluctance Machines: A Review", *IEEE Access*, vol. 10, pp. 5141–5170, 2022, doi:10.1109/ACCESS.2022.3140440.

[14] G. Fang, F. P. Scalcon, D. Xiao, R. P. Vieira, H. A. Gründling, A. Emadi, "Advanced Control of Switched Reluctance Motors (SRMs): A Review on Current Regulation, Torque Control and Vibration Suppression", *IEEE Open Journal of the Industrial Electronics Society*, vol. 2, pp. 280–301, 2021, doi:10.1109/OJIES.2021.3076807.

[15] D. Torrey, "Switched reluctance generators and their control", *IEEE Transactions on Industrial Electronics*, vol. 49, no. 1, pp. 3–14, 2002, doi:10.1109/41.982243.

[16] C. Mademlis, I. Kioskeridis, "Optimizing performance in current-controlled switched reluctance generators", *IEEE Transactions on Energy Conversion*, vol. 20, no. 3, pp. 556–565, 2005, doi:10.1109/TEC.2005.852960.

[17] I. Kioskeridis, C. Mademlis, "Optimal efficiency control of switched reluctance generators", *IEEE Transactions on Power Electronics*, vol. 21, no. 4, pp. 1062–1071, 2006, doi:10.1109/TPEL.2006.876827.

[18] I. Kioskeridis, C. Mademlis, "A Unified Approach for Four-Quadrant Optimal Controlled Switched Reluctance Machine Drives With Smooth Transition Between Control Operations", *IEEE Transactions on Power Electronics*, vol. 24, no. 1, pp. 301–306, 2009, doi:10.1109/TPEL.2008.2005983.

[19] Y. Sozer, D. Torrey, "Closed loop control of excitation parameters for high speed switched-reluctance generators", *IEEE Transactions on Power Electronics*, vol. 19, no. 2, pp. 355–362, 2004, doi:10.1109/TPEL.2003.823178.

[20] W. R. H. Araujo, M. R. C. Reis, G. A. Wainer, W. P. Calixto, "Efficiency Enhancement of Switched Reluctance Generator Employing Optimized Control Associated with Tracking Technique", *Energies*, vol. 14, no. 24, 2021, doi:10.3390/en14248388.

[21] T. A. Barros, P. J. Neto, P. S. Filho, A. B. Moreira, E. Ruppert, "Approach for performance optimization of switched reluctance generator in variable-speed wind generation system", *Renewable Energy*, vol. 97, pp. 114–128, 2016, doi:https://doi.org/10.1016/j.renene.2016.05.064.

[22] W. R. H. Araújo, C. A. Ganzaroli, W. P. Calixto, A. J. Alves, G. P. Viajante, M. R. C. Reis, A. F. V. Silveira, "Firing angles optimization for Switched Reluctance Generator using Genetic Algorithms", *in 2013 13th International Conference on Environment and Electrical Engineering (EEEIC)*, pp. 217–222, 2013, doi:10.1109/EEEIC-2.2013.6737911.

[23] L. Ge, B. Burkhart, A. Klein-Hessling, H. Xu, R. W. De Doncker, "Comprehensive Performance Comparison and Optimization of Single-Pulse Controlled SRGs for Renewable Electrical Grids", *in 2019 IEEE Applied Power Electronics Conference and Exposition (APEC)*, pp. 2632–2637, 2019, doi:10.1109/APEC.2019.8722170.

[24] P. J. d. S. Neto, T. A. d. S. Barros, M. V. de Paula, R. R. de Souza, E. R. Filho, "Design of Computational Experiment for Performance Optimization of a Switched Reluctance Generator in Wind Systems", *IEEE Transactions on Energy Conversion*, vol. 33, no. 1, pp. 406–419, 2018, doi:10.1109/TEC.2017.2755590.

[25] P. J. dos Santos Neto, T. A. d. S. Barros, E. H. Catata, E. R. Filho, "Grid-Connected SRG Interfaced With Bidirectional DC-DC Converter in WECS", *IEEE Transactions on Energy Conversion*, vol. 36, no. 4, pp. 3261–3270, 2021, doi:10.1109/TEC.2021.3067500.

[26] J. Kennedy, R. Eberhart, "Particle swarm optimization", *in Proceedings of ICNN'95 - International Conference on Neural Networks*, vol. 4, pp. 1942–1948 vol.4, 1995, doi:10.1109/ICNN.1995.488968.

[27] F. P. Scalcon, R. P. Vieira, H. A. Gründling, "PSO-Based Performance Optimization Procedure for Current-Controlled Switched Reluctance Generators in Wind Power Applications", *in IECON 2021 – 47th Annual Conference of the IEEE Industrial Electronics Society*, pp. 1–6, 2021, doi:10.1109/IECON48115.2021.9589390.

[28] S. M. R. Kazmi, H. Goto, H.-J. Guo, O. Ichinokura, "A Novel Algorithm for Fast and Efficient Speed-Sensorless Maximum Power Point Tracking in Wind Energy Conversion Systems", *IEEE Transactions on Industrial Electronics*, vol. 58, no. 1, pp. 29–36, 2011, doi:10.1109/TIE.2010.2044732.

[29] G. G. Koch, C. R. D. Osório, H. Pinheiro, R. C. L. F. Oliveira, V. F. Montagner, "Design Procedure Combining Linear Matrix Inequalities and Genetic Algorithm for Robust Control of Grid-Connected Converters", *IEEE Transactions on Industry Applications*, vol. 56, no. 2, pp. 1896–1906, 2020, doi:10.1109/TIA.2019.2959604.

[30] C. R. D. Osório, G. G. Koch, H. Pinheiro, R. C. L. F. Oliveira, V. F. Montagner, "Robust Current Control of Grid-Tied Inverters Affected by LCL Filter Soft-Saturation", *IEEE Transactions on Industrial Electronics*, vol. 67, no. 8, pp. 6550–6561, 2020, doi:10.1109/TIE.2019.2938474.

[31] Y. Shi, R. Eberhart, "A modified particle swarm optimizer", *in 1998 IEEE International Conference on Evolutionary Computation Proceedings. IEEE World Congress on Computational Intelligence (Cat. No.98TH8360)*, pp. 69–73, 1998, doi:10.1109/ICEC.1998.699146.

[32] R. Eberhart, Y. Shi, "Particle swarm optimization: developments, applications and resources", *in Proceedings of the 2001 Congress on Evolutionary Computation (IEEE Cat. No.01TH8546)*, vol. 1, pp. 81–86 vol. 1, 2001, doi:10.1109/CEC.2001.934374.

[33] D. Wang, D. Tan, L. Liu, "Particle swarm optimization algorithm: an overview", *Soft Computing*, vol. 22, no. 2, pp. 387–408, 2018, doi:10.1007/s00500-016-2474-6.

[34] B. Bilgin, J. Jiang, A. Emadi, *Switched Reluctance Motor Drives: Fundamentals to Applications*, CRC Press, 2019.

[35] C. R. D. Osorio, R. P. Vieira, H. A. Grundling, "Sliding mode technique applied to output voltage control of the switched reluctance generator", *in IECON 2016 - 42nd Annual Conference of the IEEE Industrial Electronics Society*, pp. 2935–2940, 2016, doi:10.1109/IECON.2016.7793709.

[36] C. R. D. Osório, F. P. Scalcon, R. P. Vieira, V. F. Montagner, H. A. Gründling, "Robust Control of Switched Reluctance Generator In Connection With a Grid-Tied Inverter", *in 2019 IEEE 15th Brazilian Power Electronics Conference and 5th IEEE Southern Power Electronics Conference (COBEP/SPEC)*, pp. 1–6, 2019, doi:10.1109/COBEP/SPEC44138.2019.9065551.

[37] F. Pinarello Scalcon, T. Smidt Gabbi, R. Padilha Vieira, H. Abílio Gründling, "Melhoria De Desempenho De Motores De Relutância Variável Via Algoritmo De Enxame De Partículas", *Eletrônica de Potência*, vol. 25, no. 4, p. 492–502, Dec. 2020, doi:10.18618/REP.2020.4.0038, URL: https://journal.sobraep.org.br/index.php/rep/article/view/309.

[38] C. R. D. Osório, F. P. Scalcon, G. G. Koch, V. F. Montagner, R. P. Vieira, H. A. Gründling, "Controle Robusto Aplicado a Geradores de Relutância Variável Conectados à Rede", *Eletrônica de Potência*, vol. 25, no. 3, p. 272–282, Sep. 2020, doi:10.18618/REP.2020.3.0015, URL: https://journal.sobraep.org.br/index.php/rep/article/view/302.

BIOGRAPHIES

Filipe P. Scalcon received the B.Sc. (Hons), M.Sc., and Ph.D. degrees in electrical engineering from the Federal University of Santa Maria (UFSM), Santa Maria, Brazil, in 2017, 2019, and 2021, respectively. He is currently a Postdoctoral Associate with the Department of Electrical and Software Engineering, University of Calgary, Calgary, AB, Canada. He conducted research as a Member of the Power Electronics and Control Research Group, UFSM. From 2022 to 2024, he was a Postdoctoral Fellow with McMaster Automotive Resource Centre, McMaster University, Hamilton, ON, Canada. His research interests include electrical machine drives, renewable energy conversion, microgrids, reluctance machines, and digital control. Since 2024, he is an Associate Editor of the Brazilian Power Electronics Journal.

Gustavo X. Prestes received the M.Eng. degrees from Technological Institute of Aeronautics in 2011. In 2021 he started a Ph.D degree from the Federal University of Santa Maria, at Santa Maria, RS. In 2014, he joined the Federal University of Roraima, where he is currently a professor in electrical engineering department. His research interests include real-world control applications problems, especially applied to power electronic converters and electric motor drives.

Gaoliang Fang received the B.S. and M.S. degrees from Northwestern Polytechnical University, Xi'an, China, in 2015 and 2018, respectively, and the Ph.D. degree from McMaster University, Hamilton, ON, Canada, in 2021, all in electrical engineering. He is currently an Assistant Professor with the Faculty of Sustainable Engineering, University of Prince Edward Island (UPEI), Charlottetown, PE, Canada. Before he joined the UPEI, he was a Postdoctoral Fellow with the McMaster Automotive Resource Centre, McMaster University. During his postdoctoral period, he also interned at Enedym Inc., Hamilton, ON, Canada, under the support of Mitacs Accelerate Fellowship. His research focuses on advanced drive system toward transportation electrification, especially on the advanced control of switched reluctance machines and permanent magnet synchronous machines.

Cesar J. Volpato Filho received the B.S., M.S., and Ph.D. degrees in electrical engineering from the Federal University of Santa Maria, Santa Maria, Brazil, in 2017, 2018, and 2021, respectively. He is currently a Control Engineer with Siemens Gamesa, Brande, Denmark. From 2014 to 2021, he was with the Power Electronics and Control Research Group, where he worked on research and development of high performance sensorless control of ac motors. From 2022 to 2023, he was a Postdoctoral Fellow with McMaster Automotive Resource Centre, McMaster University, Hamilton, ON, Canada, where he performed research on control of switched reluctance motors. His research interests include high performance electric machine drives and applied nonlinear control.

Hilton A. Gründling was born in Santa Maria, Brazil, in 1954. He received the B.Sc. degree from the Pontifical Catholic University of Rio Grande do Sul, Porto Alegre, Brazil, in 1977, the M.Sc. degree from the Federal University of Santa Catarina, Santa Catarina, Brazil, in 1980, and the D.Sc. degree from the Technological Institute of Aeronautics, São Paulo, Brazil, in 1995. Since 1980, he has been with the Federal University of Santa Maria, Rio Grande do Sul, Brazil, where he is currently a Titular Professor. His research interests include robust model reference adaptive control, discrete control, and control system applications.

Rodrigo P. Vieira received the B.S. degree in electrical engineering from the Universidade Regional do Noroeste do Estado do Rio Grande do Sul (Unijuí), Ijuí, Brazil, in 2007, and the M.Sc. and Dr.Eng. degrees in electrical engineering from the Federal University of Santa Maria (UFSM), Santa Maria, Brazil, in 2008 and 2012, respectively. From 2010 to 2014, he was with the Federal University of Pampa, Alegrete, Brazil. Since 2014, he has been with the UFSM, where he is currently a Professor. His research interests include electrical machine drives, electric vehicles, sensorless drives, digital control techniques of static converters, and energy systems.

Andrew M. Knight is a Professor in the Department of Electrical and Software Engineering at the University of Calgary, His research interests are in energy conversion, clean and efficient energy utilization, and integration of clean energy technologies into larger systems. He is the recipient of multiple prize paper awards from IEEE Power & Energy Society and IEEE Industry Applications Society. Dr. Knight is a P.Eng. registered in the Province of Alberta, Canada. He was President of IEEE Industry Applications Society 2023-24 and currently serves as Past President. He is a member of the IEEE Smart Cities Board of Governors, the IEEE Smart Village Governing Board, IEEE Systems Council AdCom and the Steering Committee for IEEE PES/IAS PowerAfrica Conference. He has previously been General Chair of IEEE Energy Conversion Congress and Exposition (ECCE), and the Steering Committee Chair of IEEE ECCE and IEEE International Electric Machines and Drives Conference. Dr Knight is a Fellow of the Canadian Academy of Engineering, the Engineering Institute of Canada, and the Institution of Engineering and Technology.